

62. PETROLOGY OF MAGNETIC OXIDES AT SITE 417

U. Bleil, Institut für Geophysik, Ruhr Universität Bochum, Germany
and

B. Smith, Laboratoire de Géomagnétisme, 94100 Saint-Maur-des-Fossés, France

INTRODUCTION

One of the fundamental explanations of the magnetic properties of a rock resides in the chemical nature of the minerals carrying the magnetization. As a basis of a rock magnetic study, the mineralogy of the magnetic oxides in basalts from Site 417 was studied combining microscopic examinations, thermomagnetic measurements, and electron microprobe analyses.

EXPERIMENTAL METHOD

Microscopic Examination

Ninety-eight polished sections (9 in Hole 417A, 89 in Hole 417D) were examined in reflected light and immersion oil, using a Leitz Ortholux Pol microscope. The qualitative description of the opaque phases given in Table 1 is mainly concerned with the shape, the alteration features, the size ranges, and the abundance of the magnetic minerals, that is, in a broad sense, the titanomagnetites.

Quantitative estimates of the magnetic oxides, in percentage, and their average grain sizes, were obtained on a Quantimet image analyzing device assuming rounded grains. Two points must be stressed concerning the values tabulated in Table 2. (1) The magnetic oxide content is necessarily underestimated because it cannot take into account the submicroscopic grains that may dominate the magnetic properties (Evans and Wayman, 1972). Such a discrepancy between measured and real magnetic oxide percentage was pointed out by Ryall et al. (1977). (2) Optical determination of the average grain size also encounters difficulties. Again the smallest grains are not considered, but it is also somewhat problematical to assign a grain size as the whole magnetic minerals can be fragmented into smaller ones. This is actually the case in the pillows where quenching does not allow the titanomagnetite crystals to develop fully, but where, instead, skeletal of disjointed elementary crystals are initiated along the (111) spinel planes, forced by the internal crystallographic constraints of the mineral. Another mechanism responsible for the fragmenting of the magnetic grains into smaller ones is the low temperature oxidation which produces internal stresses and consequently volume crack changes. It is thus not always clear, when measuring the grain size of the magnetic oxides, which one of the total size of the whole mineral (t.s., in Table 1) or the effective size of the elementary grains (e.s., in Table 1) must be measured in order to best represent the magnetic grain size. As a matter of fact, because internal stresses inside the grains and interaction between adjacent elementary grains cannot be evaluated optically, the visible "phys-

ical" size does not necessarily represent the "magnetic" size that is the domain state range of the magnetic grains, which can be inferred from magnetic parameter measurements (Q , J_r/J_s , H_{rc}/H_c essentially).

Table 1 also describes the relationships between magnetic and non-magnetic phases; when observed inside the titanomagnetite, the ilmenite intergrowths have been identified as trellis, composite, and/or sandwich type, according to the Buddington and Lindsley (1964) and Haggerty (1976) classifications.

Thermomagnetic Measurements

Thermomagnetic experiments (heating and cooling) were performed on two different devices, allowing the Curie temperature T_c to be determined on 74 crushed basalt samples (18 in Hole 417A, 56 in Hole 417D including Leg 52). The first equipment, a commercial device, measures the temperature dependence of the susceptibility in a 1-Oe steady field under air or argon atmosphere. The second one is a Forrer-type translation balance (as described by Nagata, 1961) working in a close to saturation field of 1800 Oe, under Argon. Cross-checks performed between the two devices and in different atmospheres proved the T_c to be the same within a few degrees, and heating and cooling curves of roughly the same aspect, provided the cooling in air, which is meaningless, was not considered. In general, better steeper heating curves were recorded in 1 Oe than in 1800 Oe because the paramagnetism contribution of both ferromagnetic and paramagnetic minerals is no longer negligible in the high fields, especially as temperatures approach the Curie temperature of the magnetic minerals. Thus, Bleil and Petersen (1977) found on Leg 37 basalts that about 40 per cent of the total magnetization at 10,000 Oe could be due to the paramagnetism of the silicates. Curie points were determined at the intersection between the decreasing slope and a zero line where no magnetization remains.

Curie temperature allows the chemical composition of the titanomagnetite to be determined only if, in the stoichiometric series, both the ulvöspinel content x and the amount of minor cations like Al are known. Thermomagnetic analyses therefore need to be combined with at least another method.

Electron Microprobe Analysis

Electron microprobe analyses of 11 samples (3 in Hole 417A, 8 in Hole 417D) were carried out on a Camebax equipment, all in the massive units where the titanomagnetite effective grain size was large enough. An average of three analyses was made per titanomagnetite crystal, and about 20 crystals were analyzed per polished section. Each analysis determines the content of Fe, Ti, Al, Mg, Mn, Cr,

TABLE 1
Microscopic Description of the Polished Sections at Site 417

417A-38-2, 8-11 cm

Numerous skeletal grains, t.s. and e.s. $\leq 5 \mu\text{m}$ (1-3 μm) in the matrix.

417A-38-2, 18-21 cm

Numerous skeletal grains, t.s. up to 15 μm (1-3 μm), e.s. 1-3 μm in the matrix.

417A-38-2, 48-51 cm

Numerous generally skeletal grains, locally larger and angular subhedral. t.s. up to 10 μm (3-4 μm), e.s. 2-4 μm often crystallized along the "fibers" of plagioclases, in a barely crystallized matrix.

417A-41-2, 68-70 cm

Either locally numerous and very small granules, often along the plagioclase rods t.s. $\leq 1-2 \mu\text{m}$ or as subhedral skeletal grains t.s. and e.s. 4-8 μm (5 μm). Presence of elongated red-stained silicate crystals, altered by iron oxide.

417A-44-1, 52-55 cm

Two generations of titanomagnetites; anhedral to subhedral grains with sometimes corroded contours and rare cracks, often in epitactic growth with the silicates. t.s. 10-200 μm (20-50 μm), e.s. 10-50 μm . Ilmenite is common in these grains, either as a set of fine trellis lamellae (in 3 directions) of high temperature exsolutions, or as external composite inclusions (5-10 μm) developed preferentially at the grain border (probably of primary origin), or as lensoidal sandwich laths, crossing the crystal. Combinations of these 3 types (especially trellis and composite type) are common. Presence of rare ilmenite laths in some silicate grains (primary ilmenite). Fine grains spread in the matrix, t.s. and e.s. around 1 μm . Presence of numerous rounded grains of primary sulfides (20-30 μm).

417A-44-1, 132-135 cm

Two generations; mainly subhedral grains with rare cracks, or fragmented corroded grains. t.s. 10-200 μm (20-100 μm), e.s. 10-70 μm . Ilmenite is common as composite inclusions (5-10 μm), mainly at the grain borders (primary ilmenite), but also inside the grains. Very little matrix with only few grains of about 1 μm in diameter, usually aligned along the silicates. The sulfides are commonly coalescent to the titanomagnetite (10-50 μm). Rare euhedral spinels.

417A-44-2, 69-72 cm

No matrix; subhedral to euhedral, well-developed titanomagnetites imbricated with the silicates. Volume change cracks are usually not very abundant. t.s. 10-300 μm (20-100 μm), e.s. 10-80 μm . Either homogeneous, or rarely showing few fine ilmenite laths crossing the crystal, or including a primary ilmenite with a graphic texture (external composite grain of ilmenite). Primary rounded sulfides.

417A-44-3, 47-50 cm

No matrix; titanomagnetites and silicates are closely imbricated; few but large homogeneous subhedral to euhedral grains with commonly epitactic overgrowths of smaller titanomagnetites along the edges of the crystals. t.s. 40-320 μm (100-200 μm), e.s. 40-80 μm . Long thin ilmenite lamellae are rare.

417A-44-3, 96-99 cm

Almost no matrix; titanomagnetites imbricated with the silicates. Few but large subhedral grains with often smaller titanomagnetites nucleated along the edges. Few volume change cracks; numerous inclusions of glass responsible for the largely corroded aspect of the grains. t.s. 50-300 μm , e.s. 5-50 μm . Very rare ilmenite, either as fine laths or as small external composite inclusions in the titanomagnetites. Seldom sharp angular fragments of titanomagnetite. t.s. and e.s. few to 10 μm . Rare rounded primary sulfides.

417D-21, CC

Rather numerous skeletal grains spread in the finely crystallized matrix. t.s. $\leq 1-30 \mu\text{m}$ (5-15 μm), e.s. $\leq 1-3 \mu\text{m}$. Sulfides are frequent (20-30 μm).

417D-22-2, 107-110 cm

Opaque minerals are rare in the red-stained areas where silicates are altered by iron oxides. They are locally numerous and tiny in the fresh matrix, preferentially concentrated along the "fibers" of hardly crystallized silicates. t.s. 2-10 μm , e.s. 1-5 μm (1-2 μm).

417D-22-4, 18-21 cm

Cruciform type of titanomagnetites, developing skeletal angular grains. Rarely subhedral. t.s. $\leq 1-60 \mu\text{m}$ (10-30 μm), e.s. $\leq 1-10 \mu\text{m}$. Sulfides are present either as secondary phase infilling the cracks of the rock, or as crystals interpenetrating the titanomagnetites.

417D-26-7, 6-9 cm

Numerous and tiny grains, again more concentrated and larger in the fresh than in the red-stained areas, preferentially developed along and between the laths of silicate germs. t.s. $\leq 1-20 \mu\text{m}$, e.s. $\leq 1-5 \mu\text{m}$ (1-3 μm). Presence of red-stained iron hydroxides.

417D-27-5, 25-27 cm

Cruciform-type titanomagnetites developing tiny skeletal grains. t.s. $\leq 1-50 \mu\text{m}$ (10-30 μm), e.s. $\leq 1-5 \mu\text{m}$.

417D-28-6, 55-58 cm

Cruciform-type titanomagnetites developing tiny skeletal grains in the matrix between the silicate grains. t.s. $\leq 1-40 \mu\text{m}$ (10-30 μm), e.s. $\leq 1-5 \mu\text{m}$. Sulfides are locally abundant as primary rounded grains (few μm) or as euhedral grains (5-30 μm) interpenetrating the titanomagnetites.

TABLE 1 – *Continued***417D-28-6, 105-108 cm**

Very tiny grains almost absent in some areas, numerous in others in the matrix. t.s. and e.s. $\leq 1.5 \mu\text{m}$ ($1.2 \mu\text{m}$).

417D-30-1, 33-36 cm

Rock at an early stage of crystallization including large areas of glass. Few visible tiny opaque grains. t.s. and e.s. $\leq 1 \mu\text{m}$. Presence of tiny dots with higher reflectivity (sulfides?).

417D-30-1, 89-92 cm

Rock at an early stage of crystallization with silicate germs. Only few visible opaque grains, either as small skeletal or as dots. t.s. $\leq 1.10 \mu\text{m}$ ($1.5 \mu\text{m}$), e.s. $\leq 1.3 \mu\text{m}$.

417D-30-4, 57-60 cm

Skeletal grains sometimes with angular shapes, often with highly jagged contours. Fine volume change cracks are visible in the largest grains. t.s. $1.30 \mu\text{m}$ ($5.20 \mu\text{m}$), e.s. $1.6 \mu\text{m}$ ($2.5 \mu\text{m}$).

417D-32-1, 62-65 cm

Rock at an early stage of crystallization including glassy areas. Rare titanomagnetites visible only in the fresh zones. t.s. and e.s. $< 1.3 \mu\text{m}$ ($\leq 1 \mu\text{m}$).

417D-32-1, 69-72 cm

Rock at an early stage of crystallization, including glass areas; few visible opaque minerals in the matrix, between the silicate germs. t.s. $\leq 1.8 \mu\text{m}$ ($1.2 \mu\text{m}$), e.s. $\leq 1.2 \mu\text{m}$.

417D-32-2, 88-91 cm

Fractured subskeletal to subhedral grains. t.s. $30.150 \mu\text{m}$ ($40.100 \mu\text{m}$), e.s. $5.30 \mu\text{m}$. Rare ilmenite as composite inclusions in the titanomagnetites. Few tiny titanomagnetites (few μm) in the rare matrix.

417D-32-3, 12-14 cm

Highly fractured subhedral to anhedral grains with numerous inclusions and shredded contours. t.s. $20.200 \mu\text{m}$ ($50.100 \mu\text{m}$), e.s. $5.30 \mu\text{m}$. Rare ilmenite developed as external composite at the grain borders. Titanomagnetites are sometimes crossed by furrows (width $2 \mu\text{m}$) of both high reflective and black granulations (metailmenite and spinel?).

417D-32-3, 44-47 cm

Subhedral slightly cracked grains, or subskeletal grains with many inclusions and fractures. t.s. $10.200 \mu\text{m}$ ($50.120 \mu\text{m}$), e.s. $5.20 \mu\text{m}$. Ilmenite rods inside the titanomagnetites are rare. Presence of subhedral grains in the rare matrix. t.s. $2.30 \mu\text{m}$ ($5.10 \mu\text{m}$), e.s. $2.10 \mu\text{m}$.

417D-32-4, 6-9 cm

Subhedral to subskeletal grains with many glassy inclusions. t.s. $30.200 \mu\text{m}$ ($30.50 \mu\text{m}$), e.s. $5.30 \mu\text{m}$. They are tightly imbricated with the silicates, sometimes in epitactic growth with them. Smaller subhedral to euhedral grains are developed along the contours of previously crystallized silicates ($5.10 \mu\text{m}$) or, more rarely, included in the silicates (few μm). Sulfides are common and essentially secondary, they are often associated to the titanomagnetites, sometimes including them as subhedral large crystals ($50.100 \mu\text{m}$) or infilling the veins of the rock.

417D-32-4, 113-116 cm

Subhedral fractured grains, sometimes intensely jagged. t.s. $10.200 \mu\text{m}$ ($50.100 \mu\text{m}$), e.s. $5.40 \mu\text{m}$. Titanomagnetites occasionally grow around an earlier silicate crystal, eventually surrounding them almost totally. Ilmenite is present but rare, either as lamellae exsolutions crossing the grains or as external composite inclusions probably of primary origin.

417D-32-5, 6-9 cm

Subhedral to euhedral finely cracked grains often with inclusions; sometimes with jagged contours. t.s. $30.100 \mu\text{m}$, e.s. $10.30 \mu\text{m}$. Ilmenite trellis lamellae of high temperature exsolutions are present but rare. Rare small titanomagnetites (few μm) underlying the silicate crystals. Presence of sulfides usually as primary rounded grains contiguous to the titanomagnetite (few μm), rarely as secondary mineral in epitactic growth on the titanomagnetites.

417D-32-5, 57-60 cm

Little cracked but highly jagged subhedral grains, often cut into shreds; imbricated with the silicates and of comparable sizes. t.s. 30.300 ($50.100 \mu\text{m}$), e.s. $2.20 \mu\text{m}$. Rare smaller grains (few μm) along the silicate borders. Sulfides are present as primary rounded grains ($5.10 \mu\text{m}$) or sometimes in large areas (up to $40 \mu\text{m}$ width).

417D-32-5, 103-106 cm

Two populations of titanomagnetites according to their degree of corrosion, covering about the same size range. Subhedral to euhedral, homogeneous, little cracked titanomagnetites sometimes with overgrowths of smaller epitactic grains along the crystal edges. Corroded and intensely cracked grains with glassy inclusions. t.s. $5.200 \mu\text{m}$ ($30.100 \mu\text{m}$), e.s. $5.40 \mu\text{m}$ ($10.20 \mu\text{m}$). Ilmenite is present either as fine sandwich-type rods crossing, partially or totally, the grain, or as external composite areas developed at the grain borders. Primary rounded sulfides are present.

417D-32-6, 6-9 cm

Subhedral, little cracked grains with inclusions of glass and frequent epitactic growth of smaller titanomagnetites on the crystal edges. t.s. $30.300 \mu\text{m}$ ($60.80 \mu\text{m}$), e.s. $10.50 \mu\text{m}$. Fine ilmenite lamellae of high temperature exsolution are present but rarely observed. Few smaller grains (few μm) crystallized between the silicates and along their edges. Sulfides are widespread, usually as subhedral grains coalescent to the titanomagnetites, rarely including small titanomagnetite grains.

TABLE 1 – *Continued***417D-32-6, 116-119 cm**

Subhedral, highly fractured and cracked grains with corroded outlines and numerous inclusions. t.s. 50-330 μm (100-150 μm), e.s. few-20 μm . Rare smaller angular grains between the silicates (few-10 μm). Ilmenite is rare, either as traces of lamellae in the titanomagnetites, or as isolated grains contiguous to the titanomagnetites. Sulfides are usually associated with the titanomagnetites, sometimes surrounded by them.

417D-32-7, 11-14 cm

Subhedral, slightly cracked to anhedral fractured grains, with jagged outlines and inclusions. Rarely subskeletal. t.s. 30-230 μm (100-150 μm), e.s. few-40 μm (5-20 μm). Rare ilmenite, as exsolution lamellae, and/or as external composite grains probably of primary origin. Few smaller grains (\leq 1-15 μm) concentrated in the rare matrix along the silicates, sometimes in crystallographic continuity with the larger titanomagnetite grains. The sulfides commonly develop subhedral large crystals (50-100 μm) sometimes with rectilinear contacts with a contiguous titanomagnetite (primary sulfide?), or infilling the veins of the rock, eventually fragmenting an early formed titanomagnetite grain (sulfide of secondary origin).

417D-33-1, 41-44 cm

A few locally concentrated subhedral to anhedral titanomagnetites with few volume change cracks, but intensely and finely jagged contours and numerous inclusions of glass or silicates. Sometimes epitactic growths of smaller titanomagnetites on larger ones. t.s. 5-150 μm (50-100 μm), e.s. few-40 μm (5-10 μm). Very rare laths of ilmenite in few titanomagnetites. Few titanomagnetites of 10-15 μm . Presence of a red-stained iron hydroxide (?) in large anhedral crystals (40-150 μm) which seems to replace earlier formed silicates; it sometimes surrounds primary rounded grains of sulfide.

417D-33-1, 134-137 cm

Anhedral to subskeletal grains with numerous cracks and glassy inclusions. t.s. 30-200 μm (80-120 μm), e.s. 1-30 μm (5-15 μm). Few grains of few μm diameter. Ilmenite is present but not widespread, as external composite inclusions (10-20 μm) on the titanomagnetite edges, as sandwich type laths associated with the titanomagnetite, and as isolated subhedral grains (5-10 μm) usually close to the titanomagnetites. The last two types are of primary origin.

417D-33-2, 55-57 cm

A few subhedral, finely cracked grains with numerous small inclusions. Sometimes epitactic growth of smaller titanomagnetites on larger ones. t.s. 60-200 μm (100-150 μm), e.s. 1-40 μm (5-20 μm). Rare ilmenite in the titanomagnetites, as fine and rare lamellae, or as small areas (5-10 μm) of composite type. Numerous rounded grains of primary sulfide.

417D-33-2, 111-114 cm

A few locally concentrated subhedral to anhedral grains with jagged outlines and numerous glassy inclusions and volume change cracks. t.s. 20-150 μm (40-100 μm), e.s. 1-30 μm . Rare ilmenite in the titanomagnetite, as fine (exsolution?) lamellae or as areas of composite type. Rare smaller grains (5-10 μm) around the silicates. Sulfides are locally widespread as subhedral grains contiguous to the titanomagnetites (20-40 μm), or infilling the veins of the rock (secondary sulfide).

417D-33-3, 27-30 cm

In this rock sample all the crystals are fractured (stress effects?). A few, locally concentrated anhedral to subhedral intensely jagged and cracked titanomagnetites, with numerous small angular inclusions. t.s. 30-300 μm (50-100 μm), e.s. 1-20 μm (few μm). They are frequently in epitactic growth with the silicates. Very few of them, with rounded outlines (\sim 100 μm) are partially or totally included in a silicate (rests of intratelluric crystals?). Few angular titanomagnetites (5-20 μm) in the rare matrix. Sulfides are developed as large grains (50-150 μm) or as secondary minerals in the veins of the rock, sometimes fragmenting a titanomagnetite grain.

417D-33-3, 74-77 cm

Relatively few grains of subhedral, finely cracked titanomagnetite with abundant inclusions of various sizes. Epitactic growth of smaller titanomagnetites is developed on the most compact grains. t.s. 40-300 μm (50-120 μm), e.s. 2-30 μm (5-10 μm). Few angular grains (1-10 μm) wedged between the olivine crystal edges. Ilmenite is quite common either as isolated grains close to the titanomagnetites, or inside the titanomagnetites; in this case, they can form a set of exsolution lamellae, or sandwich type laths with non-parallel and diffuse edges, or small areas (5-10 μm) of composite type either internal, or external with a graphic texture.

417D-33-4, 27-30 cm

Subskeletal to euhedral homogeneous little cracked titanomagnetites. t.s. 30-300 μm (50-100 μm), e.s. 5-80 μm (10-20 μm). Rare ilmenite areas (\approx 10 μm) of composite type inside the titanomagnetites. Rare angular fragments of titanomagnetite (few μm). Sulfides are often rounded homogeneous grains (5-10 μm), or larger subhedral crystals (30-50 μm) with an exsolution network.

417D-33-4, 77-80 cm

Subhedral, fractured and cracked titanomagnetites with numerous inclusions. t.s. 30-250 μm (50-100 μm), e.s. 2-25 μm (10 μm). Rare traces of ilmenite lamellae, or external composite inclusions of primary ilmenite in the titanomagnetites. Few smaller grains (2-10 μm) in the rare matrix around the other minerals.

417D-33-4, 132-135 cm

Subhedral, moderately cracked titanomagnetites with glassy inclusions and sometimes epitactic overgrowths of smaller ones along the crystals' edges. t.s. 20-200 μm (50-80 μm), e.s. few-40 μm (5-20 μm). Ilmenite is present in some titanomagnetites, but not common as traces of fine lamellae or as external composite inclusions elongated along the grain borders. Less numerous smaller angular to euhedral grains (\leq 1-10 μm) in the matrix, along the silicate edges. Presence of sulfides in subhedral crystals, rarely infilling the veins.

TABLE 1 – *Continued***417D-33-5, 29-32 cm**

Subhedral to euhedral moderately cracked grains with few glassy inclusions and sometimes epitactic overgrowths of smaller titanomagnetites on the grain edges. t.s. few-250 μm (50-80 μm), e.s. few-40 μm (10-20 μm). Ilmenite is present, rarely as (exsolution?) lamellae parallel to crystal edges, more often as external composite inclusions (of primary origin?) with irregular contours (10-40 μm) developed on the grain borders; also as independent grains. The sulfides are anhedral, with granular exsolutions, and are often contiguous to a titanomagnetite or an ilmenite grain.

417D-33-5, 75-78 cm

Most often anhedral, intensely jagged grains with numerous glassy inclusions. t.s. all sizes up to 150 μm (50-100 μm), e.s. 1-20 μm . Some of the smallest angular grains ($\leq 1.5 \mu\text{m}$) can be included in silicate grains. Ilmenite is rare, as external composite inclusions on the edges of the titanomagnetites. Presence of a red-stained subhedral and jagged iron hydroxide (?) (50-80 μm).

417D-33-6, 22-25 cm

All the minerals of this section are cracked and partially crushed, maybe as a result of stress effects. Subhedral to anhedral, highly corroded titanomagnetites with numerous inclusions, often dissociated into several fragments. t.s. 20-180 μm (30-50 μm), e.s. 1-20 μm (5-10 μm). Rare ilmenite laths developed in the titanomagnetites. Presence of sulfides, as rounded grains of primary origin, but more commonly as secondary mineral infilling the veins and developing large subhedral crystals around the veins and often close to the titanomagnetites.

417D-34-1, 31-34 cm

Few, generally subhedral titanomagnetites with wide volume change cracks, sometimes also with jagged contours and inclusions. t.s. 20-100 μm (30-50 μm), e.s. few-30 μm . Few angular fragments ($< 1.10 \mu\text{m}$) in the rare matrix. Few grains of primary rounded sulfide (few μm).

417D-34-1, 106-109 cm

Two populations of titanomagnetites. Subhedral to subskeletal homogeneous, moderately cracked grains, sometimes in epitactic growth with the silicates. t.s. 10-150 μm (30-40 μm), e.s. 6-30 μm (10-20 μm). Smaller grains ($< 1.5 \mu\text{m}$) concentrated in the matrix, mainly around the silicates, underlying their contours. Anhedral grains of sulfides commonly including exsolutions, often developed in the neighborhood of the titanomagnetites.

417D-34-2, 25-28 cm

Two clearly distinct populations. Subhedral to subskeletal titanomagnetites usually slightly cracked and homogeneous, locally with small angular inclusions. t.s. 20-100 μm (40-60 μm), e.s. 5-30 μm . Numerous, tiny titanomagnetites ($\leq 1 \mu\text{m}$) mainly dispersed in the matrix or concentrated around the silicate crystals; rarely included in silicates.

417D-34-2, 126-129 cm

Two clearly distinct populations. Subhedral to subskeletal fractured and cracked titanomagnetites with few glassy inclusions. t.s. 20-120 μm (30-50 μm), e.s. 5-30 μm . Much smaller grains ($< 1.2 \mu\text{m}$) dispersed in the matrix or underlying the silicate contours. Sulfides, mainly as secondary mineral infilling the veins, and developed around and across titanomagnetite crystals.

417D-34-3, 84-87 cm

Two distinct populations. Subhedral to subskeletal cracked titanomagnetites with numerous inclusions of various dimensions. Their sizes are often comparable to those of the silicates. t.s. 30-150 μm (50-60 μm), e.s. 2-30 μm . Rather numerous small titanomagnetites ($< 1.3 \mu\text{m}$) in the matrix. One euhedral spinel grain has been seen in an olivine crystal.

417D-34-4, 20-23 cm

Two distinct populations. Subhedral to subskeletal titanomagnetites with wide volume change cracks and inclusions. In few of these grains, spots ($\approx 1 \mu\text{m}$) of anisotropic material scattered in the whole grain can hardly be seen. t.s. 30-250 μm (40-50 μm), e.s. 2-25 μm (10-20 μm). Numerous tiny grains ($< 1.3 \mu\text{m}$) dispersed in the matrix or concentrated along the silicate edges.

417D-34-4, 65-68 cm

All the dimensions of titanomagnetites up to 200 μm can be observed in this section. The larger titanomagnetites are usually subhedral to anhedral, finely jagged, with cracks and numerous glassy inclusions; they are more seldom euhedral, homogeneous, and moderately cracked. t.s. 20-200 μm (50-100 μm), e.s. few-30 μm . Smaller titanomagnetites of various sizes and shapes (1-10 μm) spread in the matrix, concentrated along the silicate edges; sometimes included in the silicates aligned along their crystallographic axes. Presence of subhedral sulfides with intergrowths.

417D-34-5, 34-37 cm

Subhedral to subskeletal titanomagnetites, moderately cracked and with few inclusions, sometimes in epitactic growth with the silicates. t.s. 10-100 μm (20-60 μm), e.s. 5-40 μm (10-20 μm). Only one trace of ilmenite lamella has been seen. Few smaller grains ($< 1.2 \mu\text{m}$) in the rare matrix or rather along the silicate edges.

417D-34-5, 83-86 cm

Skeletal titanomagnetites in dissociated elements. t.s. 1-70 μm (10-25 μm), e.s. $< 1.5 \mu\text{m}$. Sulfides sometimes interpenetrate the titanomagnetites, commonly infill the veins of the rock (secondary mineral).

417D-34-5, 100-103 cm

Numerous titanomagnetites, usually as much dislocated skeletal. t.s. 1-30 μm (5-15 μm), e.s. $< 1.4 \mu\text{m}$. Sometimes also as subhedral homogeneous grains (10-15 μm). Presence of a red-stained iron hydroxide in certain more altered areas, together with very rare subhedral hematite (?) crystals.

TABLE 1 – *Continued***417D-34-5, 117-121 cm**

Rock sample at an early stage of crystallization. Numerous tiny titanomagnetites scattered in the matrix between the grains of silicates. Generally t.s. and e.s. $\leq 1-2 \mu\text{m}$. Exceptionally skeletal grains reach $20 \mu\text{m}$ length.

417D-34-5, 124-126 cm

Usually skeletal to locally subhedral titanomagnetites. t.s. $1-30 \mu\text{m}$ ($2-10 \mu\text{m}$), e.s. $< 1-10 \mu\text{m}$.

417D-37-3, 88-91 cm

Cruciform-type titanomagnetites with skeletal to subhedral contours. t.s. $\leq 1-40 \mu\text{m}$ ($5-10 \mu\text{m}$), e.s. $\leq 1-10 \mu\text{m}$ ($\leq 1-5 \mu\text{m}$). Sulfides are common as anhedral grains (up to $30 \mu\text{m}$).

417D-37-7, 21-24 cm

Early stage of crystallization. Skeletal to subhedral tiny titanomagnetites, often underlying the rare silicate crystals contours. t.s. $\leq 1-20 \mu\text{m}$ ($1-10 \mu\text{m}$), e.s. $\leq 1-5 \mu\text{m}$.

417D-38-5, 115-118 cm

Numerous intensely indented skeletal titanomagnetites. t.s. $\leq 1-20 \mu\text{m}$ (few μm), e.s. $\leq 1-5 \mu\text{m}$ ($\leq 1-2 \mu\text{m}$). More exceptionally larger subhedral to euhedral grains ($10-30 \mu\text{m}$) with rare cracks. Presence of a red-stained iron hydroxide (?) mineral.

417D-39-2, 109-112 cm

Numerous skeletal to subskeletal, rarely subhedral, titanomagnetites with commonly indented outlines and cracks visible in the largest crystals. t.s. $5-50 \mu\text{m}$ ($10-30 \mu\text{m}$), e.s. $1-10 \mu\text{m}$. Rounded granules of primary sulfides ($5-30 \mu\text{m}$) are common in the matrix or in contact with the titanomagnetite.

417D-39-3, 31-34 cm

All sizes of titanomagnetites between ≤ 1 to $100 \mu\text{m}$, corresponding to two distinct populations. "Multiple cross arm" type skeletal indented titanomagnetites, rarely subhedral, with few fine volume change cracks; sometimes as large as the silicate grains. t.s. $10-100 \mu\text{m}$ ($20-40 \mu\text{m}$), e.s. $3-15 \mu\text{m}$. Subsequently crystallized; smaller grains spread in the matrix, locally abundant, usually $\leq 1 \mu\text{m}$.

417D-39-3, 39-42 cm

Two distinct populations. Subhedral little cracked titanomagnetites usually indented. t.s. $5-90 \mu\text{m}$ ($20-30 \mu\text{m}$), e.s. $5-20 \mu\text{m}$. Smaller grains in the rare matrix, often around the silicates (≤ 1 -few μm).

417D-39-5, 48-51 cm

Early stage of crystallization. Skeletal grains scattered in the matrix, never in the glassy areas. t.s. $\leq 1-20 \mu\text{m}$ ($5-10 \mu\text{m}$), e.s. $\leq 1-4 \mu\text{m}$.

417D-39-5, 57-60 cm

Essentially glass, or barely crystallized rock; nothing can be seen but a few aggregates of sulfides (?) ($1-3 \mu\text{m}$).

417D-39-5, 66-69 cm

Rare, tiny grains dispersed in the matrix, preferentially in the freshest areas. t.s. and e.s. ≤ 1 -few μm . Sulfides are more commonplace than titanomagnetites, either as tiny granules ($1-3 \mu\text{m}$) associated to the titanomagnetites, or as large anhedral grains ($10-20 \mu\text{m}$) including a framework of granulous exsolutions.

417D-40-1, 37-40 cm

Numerous relatively large cruciform-type titanomagnetites, usually with jagged skeletal shape. t.s. $1-70 \mu\text{m}$, e.s. $\leq 1-10 \mu\text{m}$ ($4-5 \mu\text{m}$). Sulfides are sometimes imbricated with the titanomagnetites.

417D-41-1, 109-118

Early stage of crystallization (hyalocrystalline texture). Rare, tiny magnetic minerals locally concentrated around the germs of silicate. t.s. $\leq 1-5 \mu\text{m}$, e.s. $\leq 1-2 \mu\text{m}$. Very rarely as euhedral grains of $\approx 10 \mu\text{m}$. Numerous rounded grains of primary sulfides (few μm).

417D-41-5, 50-52 cm

Subskeletal titanomagnetites with inclusions and few volume change change cracks. t.s. $5-100 \mu\text{m}$ ($20-30$ -), e.s. $2-20 \mu\text{m}$. Very few grains in the rare matrix ($\leq 1 \mu\text{m}$), rarely included in silicates.

417D-41-6, 18-21 cm

Hardly crystallized rock. Cruciform-type titanomagnetites in fine skeletal. t.s. $1-50 \mu\text{m}$, e.s. $\leq 1-8 \mu\text{m}$ ($2-5 \mu\text{m}$). Rather common primary sulfides associated to the titanomagnetites.

417D-42-1, 64-67 cm

Early stage of crystallization (subhyalocrystalline texture). The magnetic minerals, almost absent in the red-stained zones, are numerous and scattered in the "fresh" gray areas, usually as spots, rarely as small skeletal. t.s. $\leq 1-7 \mu\text{m}$, e.s. $\leq 1 \mu\text{m}$.

TABLE 1 – *Continued***417D-42-1, 105-107 cm**

Rather well crystallized pillow. Skeletal titanomagnetites with few cracks visible in the largest elements. t.s. $\leq 1-150 \mu\text{m}$ (20-50 μm), e.s. $\leq 1-15 \mu\text{m}$ (5-10 μm).

417D-42-6, 127-130 cm

Cruciform-type titanomagnetites in very indented skeletal. t.s. $\leq 1-30 \mu\text{m}$, e.s. $\leq 1-8 \mu\text{m}$ ($\leq 1-3 \mu\text{m}$). Presence of rounded primary sulfides (few μm).

417D-43-3, 21-24 cm

Subhedral to subskeletal, highly indented and fractured grains. t.s. 10-100 μm (20-50 μm), e.s. 5-20 μm . Rare isolated crystals of ilmenite close to the titanomagnetites. Locally, numerous tiny grains ($\leq 1 \mu\text{m}$) in the rare matrix. Presence of sulfides.

417D-43-3, 63-66 cm

Locally concentrated subskeletal to subhedral titanomagnetites with jagged contours, cracks, and large glassy inclusions. t.s. 10-70 μm (20-40 μm), e.s. 2-20 μm . Smaller grains ($\leq 1 \mu\text{m}$) scattered in the rare matrix. Rare isolated subhedral crystals of ilmenite. Sulfides are present as primary rounded grains (1-10 μm) also commonly as anhedral to subhedral crystals (30-100 μm) around the titanomagnetites, or infilling the veins of the rock. Presence of a red-stained iron hydroxide (?).

417D-43-3, 93-96 cm

Subhedral to subskeletal intensely and finely corroded titanomagnetites, with many small inclusions. t.s. 10-200 μm (30-80 μm), e.s. $\leq 1-30 \mu\text{m}$ (5-20 μm). Rather numerous smaller grains (≤ 1 -few μm) scattered in the rare matrix, or concentrated around the silicates. Presence of a red-stained iron hydroxide in large subhedral grains (50-200 μm).

417D-43-5, 93-95 cm

Usually subskeletal, sometimes subhedral intensely jagged titanomagnetites. t.s. 5-100 μm (20-40 μm), e.s. few-30 μm . Smaller grains ($\leq 1-4 \mu\text{m}$) in the matrix. Primary rounded grains of sulfides (few-10 μm). Presence of a red-stained mineral in large areas (up to 500 μm).

417D-43-6, 13-15 cm

Cruciform type titanomagnetites in dissociated skeletal. t.s. $< 1-50 \mu\text{m}$ (10-20 μm), e.s. $< 1-7 \mu\text{m}$.

427D-44-1, 37-40 cm

Numerous and rather large, finely but intensely jagged skeletal titanomagnetites, with sizes comparable to those of the silicates. t.s. $< 1-50 \mu\text{m}$ (5-30 μm), e.s. $< 1-10 \mu\text{m}$ ($< 1-5 \mu\text{m}$) Presence of a red-stained mineral (iron hydroxide?).

417D-44-1, 46-49

Rare titanomagnetites in the red-stained areas, numerous in the fresh gray zones of the matrix, with very jagged skeletal contours. t.s. $< 1-70 \mu\text{m}$, e.s. $< 1-10 \mu\text{m}$ (2-5 μm).

417D-44-2, 81-84 cm

Numerous skeletal very fragmented titanomagnetites. t.s. $< 1-30 \mu\text{m}$ (3-15 μm), e.s. $< 1-10 \mu\text{m}$ ($\leq 1-5 \mu\text{m}$).

417D-44-5, 3-6 cm

Numerous titanomagnetites in highly fragmented skeletal grains. t.s. $\leq 1-60 \mu\text{m}$ (10-30 μm), e.s. $\leq 1-10 \mu\text{m}$ (1-5 μm). Sulfides are common (of primary origin?).

417D-45-1, 27-30 cm

Numerous skeletal titanomagnetites. t.s. $< 1-30 \mu\text{m}$ (3-10 μm), e.s. $< 1-8 \mu\text{m}$ (2-5 μm).

417D-45-2, 16-19 cm

Early stage of crystallization. Titanomagnetites in highly fragmented skeletal grains. t.s. $< 1-10 \mu\text{m}$, e.s. $< 1-2 \mu\text{m}$.

417D-48-5, 38-41 cm

Two distinct populations. Numerous subhedral to subskeletal finely cracked homogeneous titanomagnetites. t.s. 5-150 μm (20-50 μm), e.s. 5-20 μm . Numerous tiny grains ($\leq 1 \mu\text{m}$) in the rare matrix.

417D-49-1, 21-23 cm

Numerous titanomagnetites, either subskeletal and little cracked, or subhedral with inclusions, finely but intensely jagged, sometimes heterogeneous, including fine exsolutions of ilmenite lamellae visible in a framework of 3 directions. Ilmenite is also present as few parallel narrow rods starting from the edges (of a grain) and interrupted near the middle of the grain. t.s. few-100 μm (10-30 μm), e.s. few-10 μm . Presence of a red-stained mineral (iron hydroxide?). Presence of primary rounded sulfides (few μm).

417D-50-2, 65-67 cm

The size range spreads between ≤ 1 to 300 μm ; 2 populations of titanomagnetites. Homogeneous subskeletal to subhedral titanomagnetites with numerous fine cracks, sometimes in epitaxial growth with the silicates. t.s. 5-300 μm (40-100 μm), e.s. 10-40 μm . Smallest grains are sometimes surrounded by subsequent silicates. Smaller grains ($\leq 1-2 \mu\text{m}$) spread in the matrix, often underlying the silicate borders. Sulfides are rare in rounded grains (10-20 μm), but common as secondary mineral infilling the veins and fragmenting an earlier formed titanomagnetite.

TABLE 1 – *Continued***417D-54-2, 135-137 cm**

Numerous, highly fragmented skeletal titanomagnetites in a subophitic textured pillow. t.s. $\leq 1-40 \mu\text{m}$ (5-20 μm), e.s. $\leq 1-4 \mu\text{m}$ (1-2 μm). Sulfides are widespread either as small primary granules (few μm) or in large subhedral areas (few-50 μm) in the rock, or imbricated with the titanomagnetites, or more seldom in the veins (secondary mineral).

417D-35-4, 87-89 cm

Ophitic texture with magnetic minerals covering all the sizes between ≤ 1 to 120 μm . Cruciform type homogeneous titanomagnetites with subskeletal to subhedral contours and fine volume change cracks visible in the largest areas. t.s. $\leq 1-120 \mu\text{m}$ (20-60 μm), e.s. $\leq 1-20 \mu\text{m}$ (1-15 μm). Presence of sulfides either as rounded granules (2-5 μm) usually close to the titanomagnetites, or as subhedral areas (10-40 μm) of secondary origin, commonly growing through an earlier crystallized titanomagnetite.

417D-59-6, 33-35 cm

Rather numerous subhedral to subskeletal homogeneous finely cracked titanomagnetites (in a subophitic texture). t.s. few-60 μm (15-30 μm), e.s. 1-20 μm .

417D-62-7, 34-37 cm

Early stage of crystallization. Tiny magnetic minerals concentrated along the silicate germs. t.s. $\leq 1-10 \mu\text{m}$ (1-6 μm), e.s. $\leq 1-4 \mu\text{m}$. Large abundance of isolated sulfides in anhedral to subhedral grains (few-50 μm) commonly exhibiting exsolution framework.

417D-63-2, 12-14 cm

Two populations. Subhedral to subskeletal homogeneous cracked titanomagnetites, rarely in fragmented skeletal grains. t.s. 10-150 μm (30-60 μm), e.s. few-30 μm (5-20 μm). Smaller grains in the rare matrix ($\leq 1-5 \mu\text{m}$), often concentrated along the silicate edges. Rounded grains of primary sulfides are common.

417D-63-3, 113-116 cm

Numerous subhedral to skeletal, homogeneous, little cracked titanomagnetites, concentrated along the silicate borders or scattered in the matrix. t.s. 1-60 μm (10-30 μm), e.s. $\leq 1-12 \mu\text{m}$ ($\approx 5 \mu\text{m}$).

417D-64-2, 70-72 cm

Rather exceptionally well developed titanomagnetites for a hardly crystallized pillow. The grains are numerous, subhedral to euhedral, rarely skeletal. t.s. $\leq 1-30 \mu\text{m}$ (1-8 μm), e.s. $\leq 1-10 \mu\text{m}$ (1-5 μm). In this section, one large (150 μm) eroded rounded grain of intratelluric titanomagnetite with inclusions, has been observed.

417D-65-6, 79-81

Subhedral to subskeletal homogeneous little cracked titanomagnetites. t.s. 10-200 μm (50-100 μm), e.s. 5-30 μm .

417D-66-3, 30-32 cm

Rarely euhedral, usually subhedral to subskeletal homogeneous little cracked titanomagnetites. t.s. 5-90 μm (15-40 μm), e.s. $\leq 1-25 \mu\text{m}$. Few tiny grains (≤ 1 -few μm) in the rare matrix, along the silicate edges.

417D-66-4, 111-114 cm

Subhedral titanomagnetites in a barely crystallized pillow. t.s. and e.s. $\leq 1-10 \mu\text{m}$ (1-3 μm).

417D-69-1, 106-108 cm

Rather large subhedral little cracked titanomagnetites, sometimes with few inclusions; the largest grains are sometimes fractured and broken into smaller elements. t.s. 50-350 μm (200-250 μm), e.s. 5-40 μm . Ilmenite is present inside the titanomagnetite grains, either as rare laths crossing the crystal (sandwich-type), or as external composite inclusions (20-30 μm) along the titanomagnetite edges, probably of primary origin.

417D-69-2, 35-37 cm

Very large subhedral to euhedral, little fractured and finely cracked titanomagnetites, with few rounded holes. Occasionally, overgrowths of smaller titanomagnetites on the edges of a larger euhedral grain can be observed. These magnetic minerals have sizes comparable to those of the surrounding silicates. t.s. 90-600 μm (200-400 μm), e.s. 20-100 μm . Ilmenite is frequent in different types, inside the titanomagnetites: as a set of thin parallel laths (developed in 1 or 2 directions) extending across the whole crystal or internally truncated or as coarse subhedral internal and/or external composite inclusions, sometimes in a graphic texture, with crystal edges that often parallel those of the titanomagnetite. Rare smaller euhedral grains (few-20 μm) wedged between well developed crystals of silicate. Frequency of rounded grains of primary sulfides, generally coalescent to the titanomagnetites.

Note: t.s. = total size of the magnetic oxides, in microns, e.s. = effective size of the magnetic oxides, in microns. The two numbers correspond to the minimum and maximum size observed. The value within brackets corresponds to the approximate size maximum frequency. See text for further explanations.

TABLE 2
Rock Type

Sample (Interval in cm)	Rock Type	Volume Percentage	Mean Size	T _c	x	% Ox
Hole 417A						
24-5, 22-25	P	0.8	4.2			
28-1, 50-53	P	0.4	3.4			
28-4, 44-46	P			338		
29-2, 84-87	P	<0.1	<1.0	355		
29-6, 83-85	P	0.4	4.6	376		
32-1, 56-59	P	0.4	1.6			
32-4, 54-57	P			345		
33-5, 82-85	P	0.5	3.2			
34-5, 40-43	P	1.6	8.8			
35-4, 7-9	P	0.2	2.0	378		
35-4, 106-109	P			343		
37-3, 23-25	P	0.7	3.0	353		
37-3, 107-110	P	0.7	2.4			
38-2, 8-11	P	0.3	1.8			
38-2, 18-21	P	1.3	2.2			
38-2, 28-31	P	0.3	2.2	376		
38-2, 38-41	P	0.2	1.8			
38-2, 48-51	P	1.1	1.8			
38-4, 34-37	P	0.2	1.0			
38-4, 49-51	P			374		
39-1, 37-40	P	2.5	6.4	346		
39-4, 81-83	P	0.3	2.0			
40-3, 17-19	P			312		
40-4, 67-69	P	0.9	2.6			
41-1, 103-105	P	2.0	6.0	291		
41-2, 68-70	P	0.5	1.2	352		
41-4, 136-139	P	0.3	3.8	311		
41-5, 144-147	P	0.7	7.8			
43-2, 25-28	P	0.7	2.6			
43-3, 118-121	M	1.2	4.8			
43-4, 27-30	M	1.5	7.0	211		
43-4, 105-108	M	1.6	15.4			
43-4, 132-135	M	0.9	8.4			
44-1, 52-55	M	1.8	11.6	382		
44-1, 83-86	M	1.3	10.2			
44-1, 132-135	M	1.5	12.2		0.58	98.8
44-2, 69-72	M	2.4	21.6		0.64	97.5
44-3, 8-11	M	2.0	20.0	197		
44-3, 47-50	M	3.0	27.4		0.63	99.4
44-3, 96-99	M	3.1	31.0			
46-1, 56-59	P	0.4	3.0	405		
Hole 417D						
21, CC	P	0.4	2.0			
22-2, 107-110	P	<0.1	<1.0	369		
22-4, 18-21	P	0.5	2.8	329		
26-7, 6-9	P	<0.1	<1.0	352		
27-5, 25-27	P	0.3	2.4	329		
27-6, 86-89	P	<0.1	<1.0			
28-4, 102-104	P			271		
28-5, 135-138	P	<0.1	<1.0	405		
28-5, 140-143	P	0.3	1.2			
28-6, 55-58	P	0.6	2.8	315		
28-6, 114-117	P			340		
29-2, 40-43	P	0.1	1.6	362		
29-2, 128-131	P	<0.1	<1.0			
29-5, 9-11	P	0.2	2.4			
30-1, 33-36	P	<0.1	<1.0	370		
30-1, 89-92	P	0.1	1.8			
30-4, 57-60	P	0.6	3.0	314		
31-4, 115-118	P	<0.1	<1.0			
32-1, 62-65	P	<0.1	<1.0	368		
32-1, 69-72	P	<0.1	<1.0			

TABLE 2 - Continued

Sample (Interval in cm)	Rock Type	Volume Percentage	Mean Size	T _c	x	% Ox
Hole 417D						
32-1, 96-98	M					274
32-1, 137-140	M					247
32-2, 88-91	M	2.2	18.0			
32-3, 12-14	M	2.7	32.5	268	0.64	96.2
32-3, 44-47	M	1.4	23.8			
32-4, 6-9	M	1.8	19.2	288		
32-4, 56-58	M			232		
32-4, 113-116	M	2.0	17.2		0.64	96.3
32-5, 6-9	M	2.0	23.0			
32-5, 57-60	M	3.4	28.4	311		
32-5, 103-106	M	2.7	28.2			
32-6, 6-9	M	2.3	24.2	242		
32-6, 60-62	M			293		
32-6, 116-119	M	2.8	24.8		0.63	96.5
32-7, 11-14	M	2.8	29.2			
33-1, 41-44	M	2.4	26.0			
33-1, 84-86	M			247		
33-1, 134-137	M	2.3	26.6	268		
33-2, 55-57	M	2.4	40.4			
33-2, 111-114	M	2.6	29.6	312		
33-3, 27-30	M	2.2	33.6			
33-3, 74-77	M	2.0	23.8		0.65	97.2
33-3, 128-131	M			242		
33-4, 27-30	M	4.4	40.8			
33-4, 77-80	M	2.4	36.4			
33-4, 132-135	M	2.4	38.0			
32-5, 29-32	M	2.3	28.6			
33-5, 75-78	M	2.3	29.2			
33-5, 122-124	M			309		
33-6, 22-25	M	2.1	26.6			
34-1, 31-34	M	2.4	26.8			
34-1, 106-109	M	2.0	12.6	242		
34-2, 25-28	M	2.2	20.4			
34-2, 77-80	M			272		
34-2, 126-129	M	1.4	18.8	255	0.62	97.6
34-3, 37-40	M			295		
34-3, 84-87	M	2.4	22.0			
34-4, 20-23	M	2.1	21.8			
34-4, 65-68	M	1.6	23.8			
34-5, 34-37	M				0.55	98.7
34-5, 83-86	P	0.8	4.6	340		
34-5, 100-103	P			341		
34-5, 117-121	P	0.8	1.2	415		
34-5, 124-126	P	0.4	2.0	334		
36-1, 138-140	P			365		
37-3, 88-91	P	0.7	3.4			
37-7, 21-24	P	0.1	1.8	342		
38-5, 115-118	P	0.3	1.8			
39-2, 109-112	M			314		
39-3, 31-34	M	2.1	15.0	260	0.59	96.5
39-3, 39-42	M	2.6	15.2	254		
39-5, 48-51	P	0.2	2.2	370		
39-5, 57-60	P	<0.1	<1.0			
39-5, 66-69	P	0.1	2.6	363		
40-1, 37-40	P	0.5	3.4			
41-1, 109-112	P	<0.1	<1.0	410		
41-3, 75-78	P	0.1	1.0			
41-5, 50-52	P	1.1	8.8			
41-6, 18-21	P	0.2	2.2			
42-1, 64-67	P	<0.1	<1.0	401		
42-1, 105-107	P	0.9	5.0			
42-6, 127-130	P	1.4	2.0			
43-3, 21-24	M	1.5	10.2			
43-3, 63-66	M	1.6	17.2	330		
43-3, 93-96	M	2.6	19.6	315	0.62	96.9

TABLE 2 – Continued

Sample (Interval in cm)	Rock Type	Volume Percentage	Mean Size	T_c	x'	% Ox
Hole 417D						
43-5, 93-95	M	1.4	10.8	355		
43-6, 13-15	P	1.6	4.8			
44-1, 37-40	P	1.8	5.0			
44-1, 46-49	P	0.3	2.4	362		
44-1, 134-136	P	0.6	5.4			
44-2, 81-84	P	1.3	3.2			
44-5, 3-6	P	1.4	4.6			
45-1, 27-30	P	1.2	3.4			
45-2, 16-19	P	0.6	1.6			394
48-7, 31-33	M			335		
49-2, 72-74	M	0.7	2.0	322		
52-1, 92-94	M	1.7	32.8	305		
54-4, 55-57	P	0.6	7.2	291		
59-6, 33-35	M	0.8	11.0	353		
62-7, 34-37	P	0.5	3.4	414		
64-2, 70-72	P	0.8	3.0	335		
67-6, 12-14	M	1.1	10.4	290		
68-5, 89-92	M	3.7	41.4	261		

Note: P = pillow M = massive; mean size in microns; T_c = Curie temperature in degrees Celsius; x = ulvöspinel content of the titanomagnetite; % Ox = percentage total oxides.

and Si. All the iron is first considered to be in the Fe^{++} state; then, part of the Fe^{++} is converted into Fe^{+++} in such a way as to make a non-oxidized titanomagnetite.

Assuming that the analyzed titanomagnetite is non-oxidized, and taking into account the substitutions of minor cations to Fe, we calculate the value x' corresponding to the ulvöspinel percentage this titanomagnetite contains (number of Ti atoms associated to 4 oxygen atoms). If the mineral analyzed is actually a non-oxidized titanomagnetite, the total of the oxide percentage (% Ox) calculated from the analysis results will be 100 per cent, within the measurement precisions of the method ($98\% \leq \% \text{Ox} \leq 101\%$), and the value x' deduced from the analyses will be the value x of the original stoichiometric titanomagnetite; here, the oxidation parameter, or fraction of initial Fe^{++} converted to Fe^{+++} (O'Reilly and Banerjee, 1967), will be $z = 0$.

In contrast, if the magnetic mineral is a cation-deficient titanomagnetite, the calculated total oxide percentage will be smaller than 100 per cent, because a larger part of Fe^{++} has been in reality converted into Fe^{+++} . The value x' will probably be somewhat higher than the value x of the original titanomagnetite (the stronger the low temperature oxidation, the larger the difference between x' and x), as a result of the slight decrease of the Fe/Ti ratio which accompanies the low temperature oxidation in the natural occurring titanomagnetites (Prévot et al., 1968). These authors actually showed that, on a gradually low temperature oxidized titanomagnetite crystal, x increased from 0.79 to 0.98 from, respectively, the non-oxidized center of the grain to the strongly oxidized outer region.

Microprobe analyses thus allow the value x' of the analyzed titanomagnetite to be known and makes it possible to tell whether or not it is oxidized. Evaluation of the oxidation parameter z can be made when microprobe analyses are combined with Curie temperature (Readman and O'Reilly, 1972).

RESULTS

According to the petrologic rock type and because it also corresponds to two different groups in terms of magnetic properties, we consider separately the massive units and the pillows.

Massive Units

In the massive units (Table 1), the magnetic minerals are large (total sizes generally around 30-100 μm) and represent an appreciable volumic percentage (from 0.7 to 5.4%, usually around 2-3%; Table 2). A second generation of smaller grains (around 1 μm) is commonplace (Figures 1, 2, 3). Sometimes relatively fresh (few samples in Hole

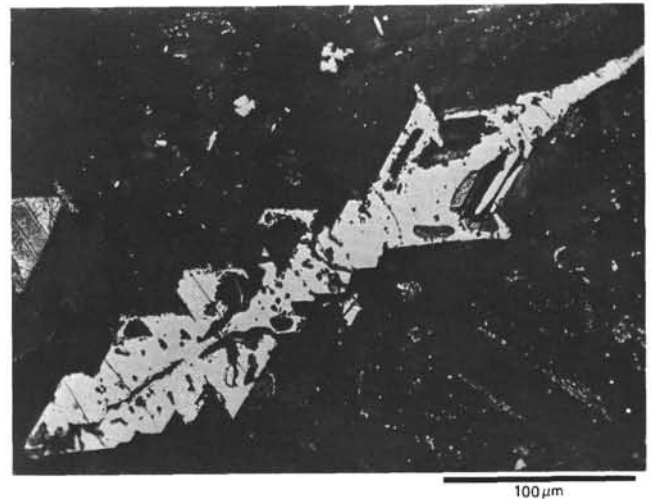


Figure 1. Large subskeletal titanomagnetite with volume change cracks among a generation of tiny ones in a sample of massive unit. Subhedral sulfide on the left of the picture. Sample 417D-34-4, 65-68 cm.



Figure 2. Multiple cross-arm type of skeletal titanomagnetite crystals among a second generation of smaller grains in a doleritic sample. Sample 417D-39-3, 31-34 cm.

417A and at the bottom of Hole 417D), the titanomagnetites are most often affected to a variable extent by volume change cracks as a result of maghemitization (Figures 4, 5, 6). No gradation of the reflectivity is seen inside the grains indicating a constant degree of oxidation. Indented contours and glassy inclusions are also common features of these minerals (Hole 417D).

Ilmenite is often observed but always in small quantities as rare isolated crystals (more seldom than in Leg 42 and 43 basalts, Petersen et al., 1978, in press), or as intergrowths inside a titanomagnetite; in this latter case ilmenite can be identified according to the Buddington and Lindsley (1964) and Haggerty (1976) classification:

1) either as internal and more often external composite inclusions the crystal edges of which often parallel those of

the titanomagnetite octahedral planes (Figures 7, 8, 9); sometimes developed in a coarse graphic texture (Figure 10) this type of ilmenite is thought to be of primary origin;

2) also as rare parallel rods developed in the (111) spinel planes, either truncated or extending throughout the crystal (Figure 11) or as large irregular lensoidal laths with non-parallel sides (sandwich type ilmenite, Figures 9, 12). In these cases, the ilmenite may be either of primary origin or may result from high temperature oxidation;

3) finally, as a network of thin lamellae exsolutions developed along the sets of (111) spinel planes, clearly of high temperature oxidation origin (trellis type Figures 13, 14, 15, 16, 17). This later type is rare in the Leg 51 massive units and, where observed, does not exceed the class 3 of the six

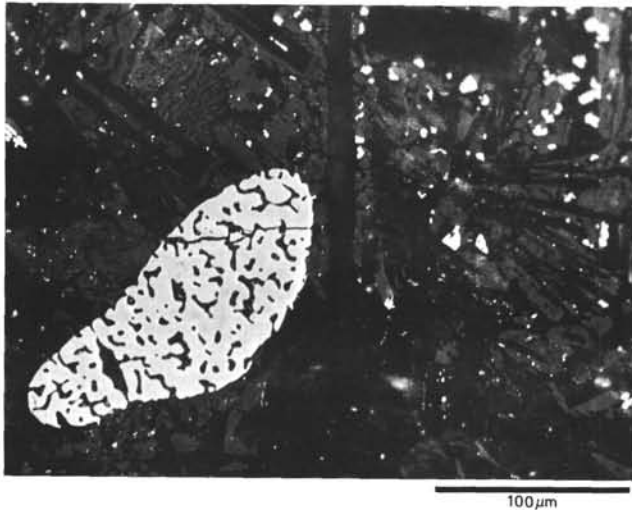


Figure 3. Remainder of an intratelluric titanomagnetite crystal among a population of smaller ones. Sample 417D-64-2, 70-72 cm.



Figure 5. Subskeletal titanomagnetite with a second generation of T-shaped crystallites nucleated along the crystal edges in a massive unit sample. Rounded sulfides (in white). Sample 417A-44-3, 96-99 cm.



Figure 4. Subskeletal to subhedral titanomagnetites with numerous volume change cracks in a massive unit sample. Presence of smaller titanomagnetite grains. Sample 417D-50-2, 65-67 cm.

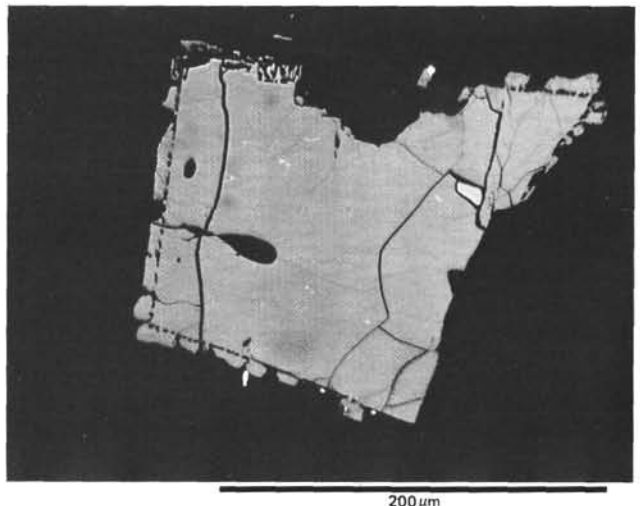


Figure 6. Subhedral titanomagnetite with few large volume change cracks and a fringe of newly formed titanomagnetite overgrowths along the edges. Sample 417D-69-2, 35-37 cm.



Figure 7. Coarse subhedral internal and external composite inclusions of ilmenite in a subhedral titanomagnetite with volume change cracks. Bright white grain of primary sulfide (polarized light). Sample 417D-69-2, 35-37 cm.

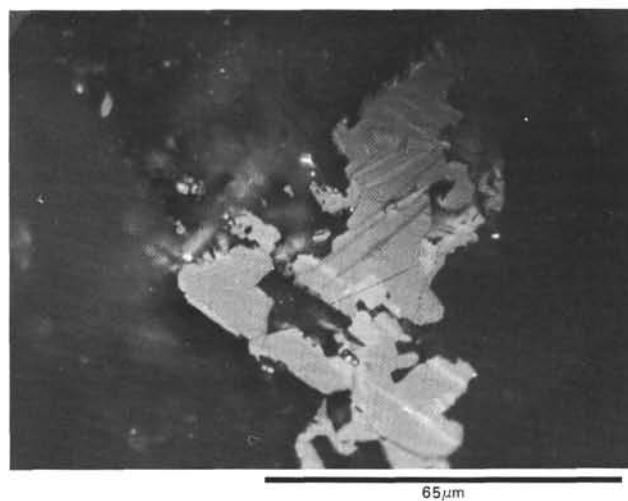


Figure 9. Anhedral titanomagnetite with ilmenite intergrowths, as lensoidal laths of sandwich type developed in the (111) spinel planes, and as external composite at the border of the titanomagnetite crystal (polarized light). Sample 417A-44-1, 52-55 cm.

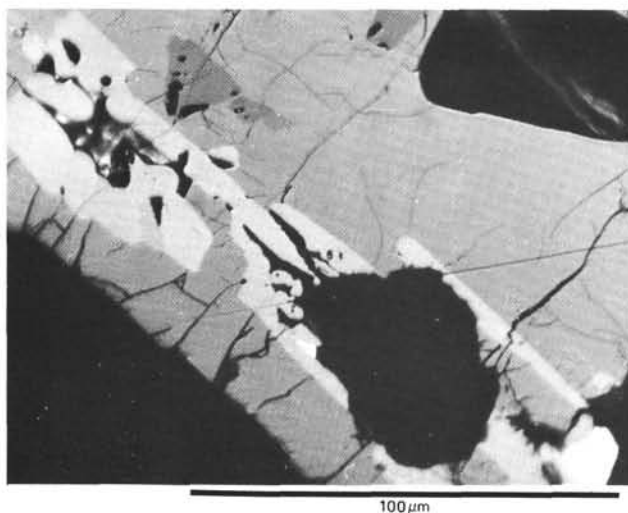


Figure 8. Detail of the ilmenite composite inclusions of the previous picture in polarized light at 90° from the former position. Sample 417D-69-2, 35-37 cm.

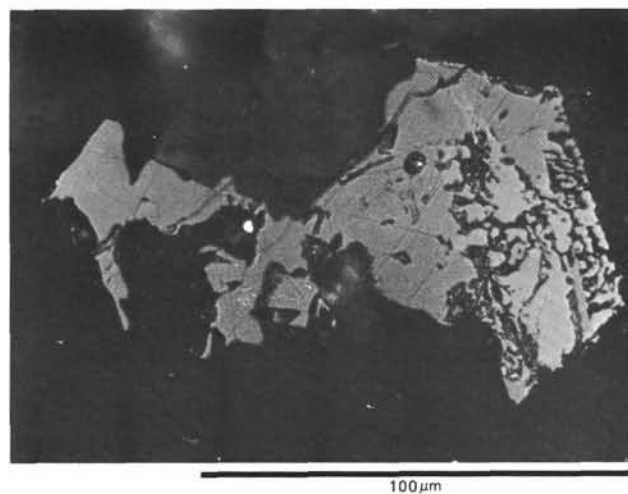


Figure 10. Subhedral titanomagnetite with external composite ilmenite crystals extending into the silicate matrix in a coarse graphic texture (polarized light). Sample 417A-44-2, 69-72 cm.

class scale of Watkins and Haggerty (1967); it is only confined to a small number of titanomagnetite crystals.

Sulfides (pyrite, chalcopyrite, and their alteration products) are common, both as primary rounded grains and as secondary minerals developed around the titanomagnetites (Figure 18) and in the cracks of the rocks (Figure 19). Although they seem to be slightly more abundant than in other DSDP legs (Leg 34, Ade-Hall et al., 1976; Legs 42 and 43, Petersen et al., 1978, in press), the sulfides are never abundant relative to the titanomagnetite volumic percentage, and thus their magnetic contribution can be reasonably neglected.

No spinel was observed, exception made for one crystal in Sample 417D-34-3, 84-87 cm.

The microprobe analyses of the 11 massive unit samples are summarized in Table 3. The values of x' cover a rather narrow composition range ($0.55 \leq x' \leq 0.65$), typical of submarine basalts (Ozima et al., 1974; Prévot and Lecaille, 1976). These values are slightly higher than the values of the original non-oxidized titanomagnetite since the magnetic minerals have undergone maghemitization to variable extent, as suggested by the total oxide percentage value ($96.2\% \leq \% \text{Ox} \leq 99.4\%$).

The amount of minor cations (Al, Mg, Mn, Cr) is lower than in subaerial basalts, but comparable to the more recent oceanic basalts of the FAMOUS area (Prévot and Lecaille, 1976).

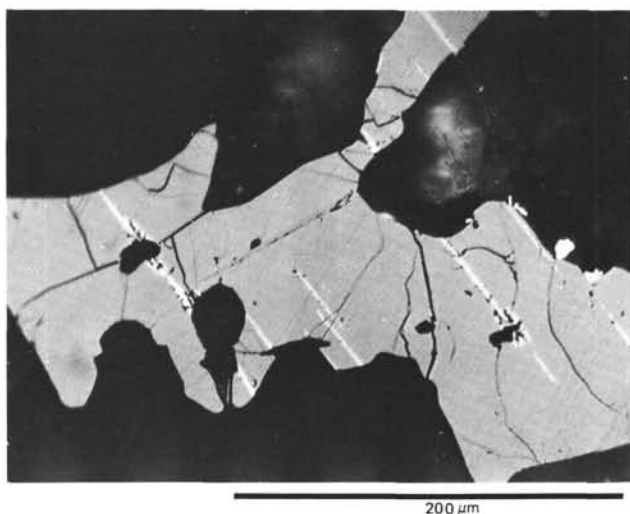


Figure 11. Titanomagnetite crystal with laths of sandwich type ilmenite, sometimes internally truncated, developed along two directions of (111) planes, in a coarse-grained sample (polarized light). Sample 417D-69-2, 35-37 cm.

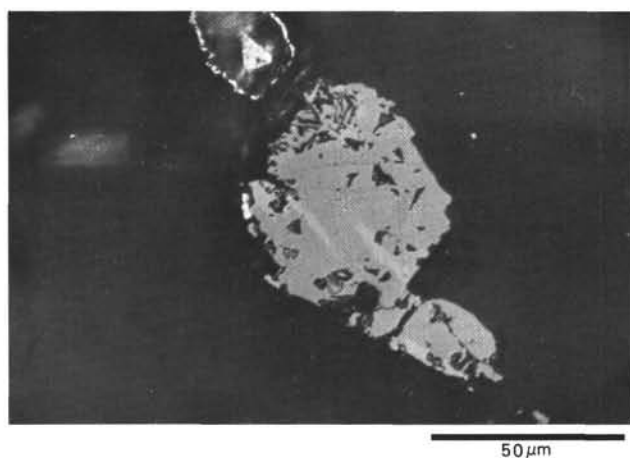


Figure 12. Anhedral titanomagnetite with glassy inclusions, with lensoidal sandwich-type ilmenite and composite-type ilmenite sometimes in a graphic texture extending into the silicate matrix. Sulfides (bright white). Polarized light. Sample 417D-33-3, 74-77 cm.

Substitution to the iron of minor cations can lower the Curie temperature of a non-oxidized titanomagnetite; this effect is particularly pronounced for aluminum but negligible for other elements (Richard et al., 1973; O'Donovan and O'Reilly, 1977). According to these first authors' experimental results, for a synthetic non-oxidized titanomagnetite of $x = 0.6$, a concentration of 0.1 atom per formula unit $\text{Fe}_{3-x}\text{Ti}_x\text{O}_4$, which is presently the average Al content, is sufficient to lower by 45°C the Curie point of the non-substituted stoichiometric titanomagnetite. Assuming that the effect of Al will be similar on a non-oxidized $x = 0.6$ titanomagnetite, and on the same but cation-deficient magnetic mineral, we determine the Curie point, T_{ce} (Table 3) one would measure if the cation-deficient titanomagnetite were not Al substituted. Combining the values x' obtained

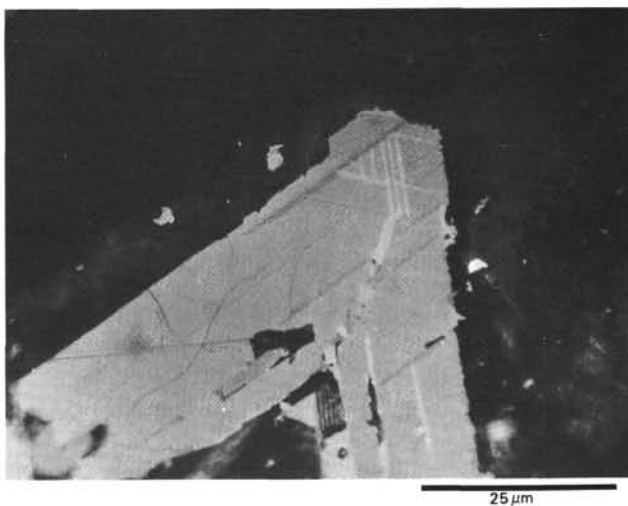


Figure 13. Subhedral titanomagnetite with ilmenite intergrowths as sets of lamellae (exsolutions?) developed in the three directions of the (111) spinel planes, and as composite inclusions inside the titanomagnetite or along its edges (polarized light). Sample 417A-44-1, 52-55 cm.

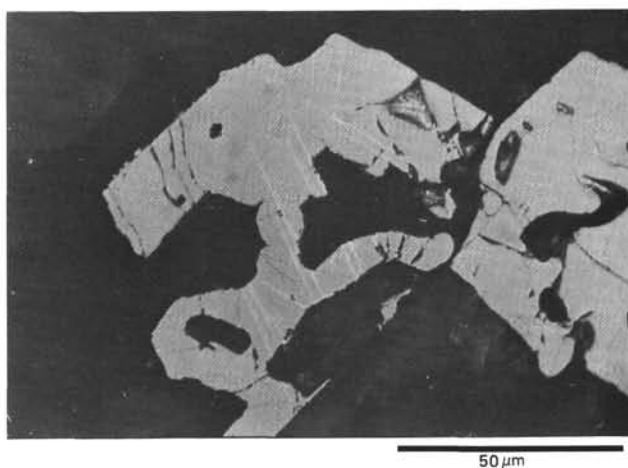


Figure 14. Subskeletal to subhedral titanomagnetite with two sets of fine ilmenite lamellae (deuteric oxidation class 2) and newly formed crystallites along the edges (polarized light). Sample 417D-32-6, 6-9 cm.

by microprobe analyses with the value T_{ce} , we determine the oxidation parameter z of the titanomagnetites present in the samples, by interpolation of the experimental curves of Readman and O'Reilly (1972) obtained on synthetic non-substituted titanomagnetites with variable degrees of cation deficiency.

Table 3 also gives the Curie temperature T_{ce} of the non-oxidized and non-substituted titanomagnetite equivalent to the value x' . The Curie points T_{ce} are drawn from the $T_c = f(x)$ curves obtained by Akimoto et al. (1957), Ghorbanian (1966), Bleil (1971), Ozima and Sakamoto (1971), and Readman and O'Reilly (1972) on synthetic non-oxidized titanomagnetites, and are determined within $\pm 30^\circ\text{C}$ for chemical composition reasons (Jensen and Shive, 1973). Therefore, we are led to admit that only if $T_{ce} \geq (T_{ce} +$

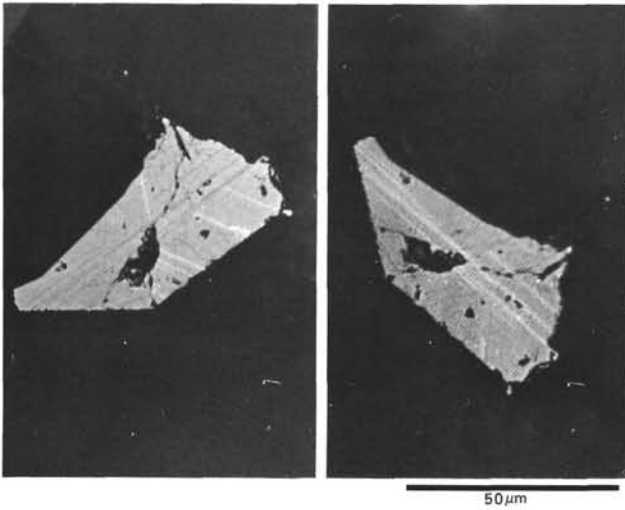


Figure 15. Subhedral titanomagnetite with three sets of ilmenite lamellae (deuteric oxidation class 2) in the (111) spinel plane. Polarized light in two positions at 90° from each other. Sample 417D-32-6, 6-9 cm.

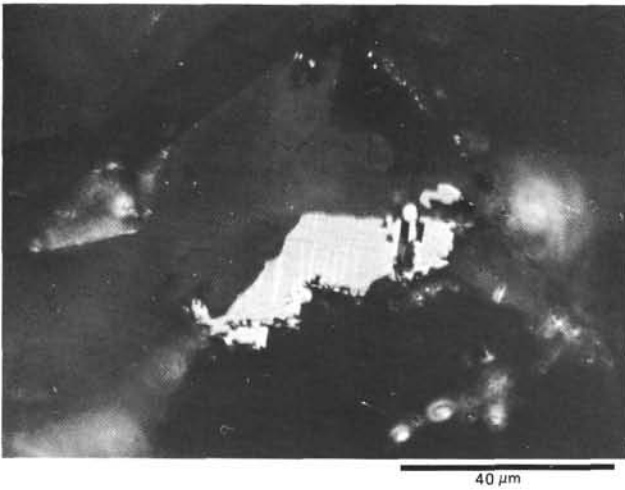


Figure 16. Euhedral titanomagnetite with two sets of ilmenite lamellae (deuteric oxidation class 3), together with external composite inclusion initiated from the crystal edges. Sample 417A-44-1, 52-55 cm.

30°C), the titanomagnetite can be held to be low temperature oxidized.

For the only four Hole 417D samples, where both Curie points and microprobe analyses were carried out, z is found to vary between $0.6 \leq z \leq 0.8$. The Curie temperatures of the massive unit samples are generally between 200° and 330°C (Table 2).

In Hole 417A, the average Curie point and the standard deviation of three samples are $\bar{T}_c = 263 \pm 84^\circ\text{C}$, and in Hole 417D, $\bar{T}_c = 285 \pm 32^\circ\text{C}$ (on 29 samples). Except for the lowermost part of Hole 417D (2 samples), a general but slight trend of increasing T_c with depth is observed when the different massive units are considered separately:

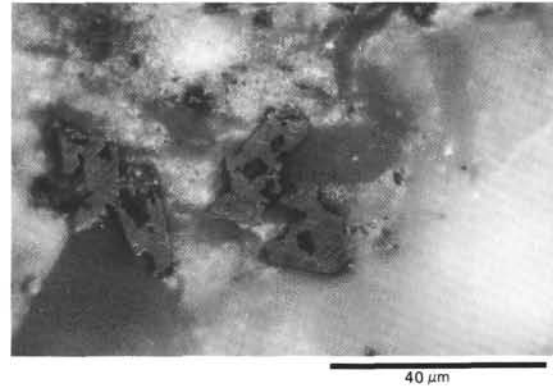


Figure 17. Euhedral titanomagnetites with ilmenite exsolution lamellae (deuteric oxidation class 3). Sample 417D-49-1, 21-23 cm.

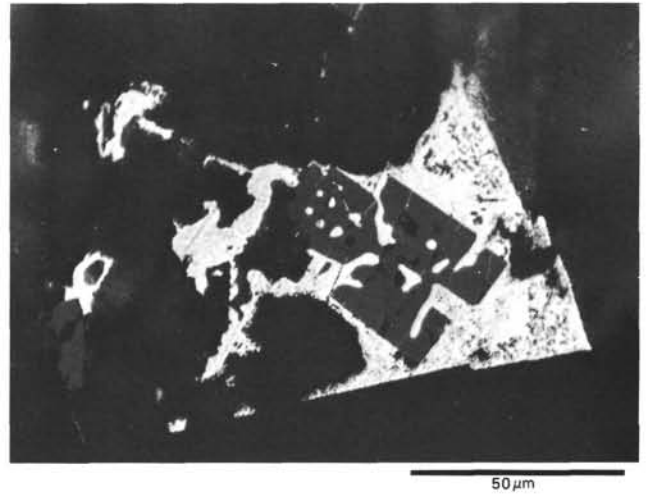


Figure 18. Subskeletal titanomagnetite included in a subhedral crystal of secondary sulfide. Sample 417D-32-4, 6-9 cm.

from 32-1, 96-98 cm to 34-3, 37-40 cm,	$\bar{T}_c = 271 \pm 26^\circ\text{C}$ (17 samples)
{ 39-2, 109-112 cm to 39-3, 39-42 cm,	$\bar{T}_c = 301 \pm 31^\circ\text{C}$ (5 samples)
and 43-3, 63-66 cm to 43-3, 93-96 cm }	
48-7, 31-33 cm to 59-6, 33-35 cm,	$\bar{T}_c = 320 \pm 21^\circ\text{C}$ (5 samples)
67-6, 12-14 cm and 68-5, 89-92 cm,	$\bar{T}_c = 276^\circ\text{C}$ (2 samples)

These values however are not significantly different.

The shape of the heating and cooling curves are rarely almost reversible (Samples 417A-43-4, 27-30 cm and 417A-44-1, 52-55 cm; 417D-32-4, 56-58 cm and 417D-68-5, 89-92 cm), but usually clearly irreversible with a more or less pronounced unmixing of the magnetic mineral upon heating. The initial intensity J_{si} before heating is always similar to the final value J_{sf} obtained after cooling. By comparison with the results obtained on synthetic cation-deficient titanomagnetite by Readman and O'Reilly (1970),

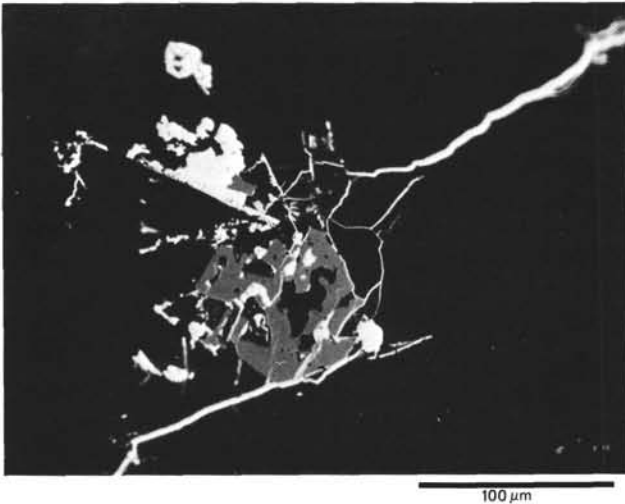


Figure 19. Secondary sulfide developed in the veins of the rock and dissociating a titanomagnetite crystal. Sample 417D-50-2, 65-67 cm.

it can be assumed that, upon heating, a natural occurring oxidized titanomagnetite will split into a ferrimagnetic spinel Fe-rich phase and one or two, depending on the initial composition of the titanomaghemite, antiferri- or paramagnetic Ti-rich phases; if, however, the ferrimagnetic newly formed mineral is more strongly magnetic than the initial titanomaghemite, it is formed in smaller quantity. It looks like these two opposing effects counterbalance each other to give a comparable J_s .

If we assume from the 11 microprobe analyses that the titanomagnetites of the massive units have everywhere a composition x of $0.55 \leq x \leq 0.65$, and an Al content around 0.1 atom per formula unit, the interpretation of the

Curie points together with the microprobe analyses data show that low temperature oxidation is commonplace in the massive units, but to variable degrees, i.e., close to zero in a few samples of Hole 417A (44-1, 52-55 cm; 44-3, 47-50 cm), z can exceed 0.8 in several samples of Hole 417D (32-5, 57-60 cm; 33-2, 111-114 cm; 33-5, 122-124 cm; 39-2, 109-112 cm; 43-3, 63-66 cm; 48-7, 31-33 cm; 52-1, 92-94 cm; 59-6, 33-35 cm).

Although microprobe analyses and thermomagnetic experiment results seem to indicate that the massive unit samples are generally slightly less oxidized in Hole 417A than in Hole 417D, this remark is based on a too small number of data in Hole 417A to be conclusive.

Pillows

The magnetic minerals of the pillows are quenched skeletal titanomagnetites, typical of submarine lava flows. They are often numerous but small (volume contents usually around 0.5 to 1 per cent, Table 2), with sizes from below the optical microscope limit to about $50 \mu\text{m}$; the largest grains are fragmented into smaller elementary grains as a result of the rapid crystallization effect, and fractured by subsequent low temperature alteration volume change cracks (Figures 20, 21, 22). Because of the too small dimensions of the titanomagnetites, no microprobe analysis was carried out in the pillows.

The Curie temperatures (Table 2) are generally higher (340° to 380°C) than in the massive units and the heating and cooling curves are always clearly irreversible.

In Hole 417A, $\bar{T}_c = 346 \pm 26^\circ\text{C}$ (14 samples). It is worth noting that most of the Hole 417A pillow samples display quite different heating and cooling curves. Precisely, the intensity of magnetization after cooling, J_{sf} , is by about an order of magnitude higher than the intensity before heating, J_{si} . The Ti-poor ferrimagnetic spinel phase formed upon

TABLE 3
Average Chemical Composition and Curie Temperature of Titanomagnetites Analyzed by Electron Microprobe

Sample (Interval in cm)	Fe	Ti	Al	Mg	Mn	Cr	Si	x'	% Ox	Al _{at}	T_{cm}	T_{cc}	T_{ce}	z
Hole 417A														
44-1, 132-135	57.0	12.3	0.8	0.2	0.4	0.01	0.1	0.58	98.8	0.06	-	-	-	-
44-2, 69-72	55.0	13.2	0.6	0.3	0.4	0.03	-	0.64	97.5	0.05	-	-	-	-
44-3, 47-50	55.6	13.5	0.9	0.5	0.4	0.02	0.2	0.63	99.4	0.07	-	-	-	-
Hole 417D														
32-3, 12-14	53.6	13.3	1.0	0.3	0.4	0.02	0.4	0.64	96.2	0.08	268	294	140	0.7
32-4, 113-116	54.1	13.2	0.9	0.2	0.4	0.02	0.2	0.64	96.3	0.07	-	-	-	-
32-6, 116-119	54.3	13.1	0.8	0.2	0.4	0.02	-	0.63	96.5	0.07	-	-	-	-
33-3, 74-77	54.4	13.5	0.8	0.2	0.4	0.02	0.2	0.65	97.2	0.07	-	-	-	-
34-2, 126-129	54.7	13.0	1.0	0.5	0.4	0.02	0.2	0.62	97.6	0.09	224	261	160	0.6
34-5, 34-37	57.8	11.5	0.7	0.3	0.3	0.02	0.1	0.55	98.7	0.06	-	-	-	-
39-3, 31-34	54.0	12.2	1.3	0.7	0.4	0.03	-	0.59	96.5	0.11	260	313	190	0.65
43-3, 93-96	53.8	12.9	1.2	0.4	0.7	0.02	0.2	0.62	96.9	0.10	315	360	160	0.8

Note: The metal contents are given in weight per cent; x' = molecular percentage of ulvöspinel in the analyzed titanomagnetite, assuming it is a pure and non-oxidized equivalent titanomagnetite (Prévoit and Mergoïl, 1973); % Ox = sum of the oxide percentages, expected to be 100% (98 to 101%) for a stoichiometric titanomagnetite (when $x = x'$); Al_{at} = concentration of Al atom per formula unit ($\text{Fe}_3 - x\text{Ti}_x\text{O}_4$); T_{cm} = measured Curie point of the substituted oxidized titanomagnetite; T_{cc} = Curie point of the corresponding oxidized non-substituted titanomagnetite (corrected for the Al content); T_{ce} = Curie point of the equivalent non-oxidized non-substituted titanomagnetite; z = oxidation parameter or fraction of Fe^{++} of the non-oxidized titanomagnetite converted to Fe^{+++} .



Figure 20. Skeletal titanomagnetites in a subophitic texture of a pillow. Sample 417D-54-2, 135-137 cm.

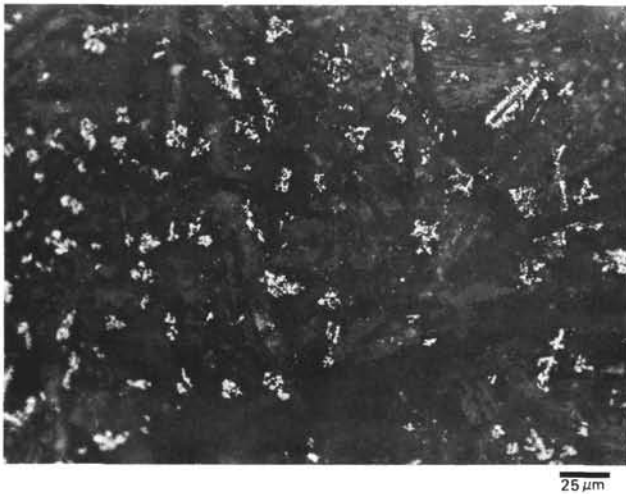


Figure 21. Skeletal titanomagnetites with indented contours in a pillow. Sample 417D-44-1, 37-40 cm.

heating is close to the magnetite composition, with an average cooling Curie point of $\bar{T}_c = 522 \pm 14^\circ\text{C}$ (10 samples). This is only a few degrees higher than that observed in the massive units and in the pillows of Hole 417D; it is possible that it does not account alone for the large difference between J_{si} and J_{sf} . From petrological examinations (this volume) the brownish color of most of the pillows in Hole 417A is attributed to the presence of widespread iron hydroxides. It is likely that, upon heating in reducing Argon atmosphere, these iron hydroxides become available to be converted into a Ti-poor titanomagnetite, thus also contributing to the large increase of the intensity of magnetization recorded after cooling.

In Hole 417D, $\bar{T}_c = 358 \pm 34^\circ\text{C}$ (27 samples). As for the massive units of Hole 417D, a slight trend of increasing T_c with depth is observed when the pillowed flows separated by the massive units are considered:



Figure 22. Cruciform-type titanomagnetites in a pillow. Sample 417D-41-6, 18-21 cm.

from 22-2, 107-110 cm to 32-1, 69-72 cm, $\bar{T}_c = 344 \pm 34^\circ\text{C}$ (12 samples)
 from 34-5, 83-86 cm to 37-7, 21-24 cm, $\bar{T}_c = 356 \pm 28^\circ\text{C}$ (6 samples)
 from 39-5, 48-51 cm to 45-2, 16-19 cm, $\bar{T}_c = 379 \pm 20^\circ\text{C}$ (7 samples)
 62-7, 34-37 cm and 64-2, 70-72 cm, $\bar{T}_c = 375^\circ\text{C}$ (2 samples)

As in the case of Hole 417D massive units, these values are not significantly different. Here, the irreversible thermomagnetic curves resemble those of the massive units with $J_{sf} \approx J_{si}$.

If, as for the 11 analyzed massive unit samples, the magnetic minerals of the pillows are cation-deficient titanomagnetites, of average original stoichiometric composition $x = 0.6$, which is a reasonable assumption for submarine basalts so far studied (Prévot and Lecaille [1976], Ade-Hall et al. [1976a], Bleil and Petersen [1977]), and assuming a similar mean Al content of 0.1 atom/formula unit, the values of z obtained from the Curie temperature (Readman and O'Reilly, 1972) cover the range of $0.7 \leq z \leq 0.95$ in Hole 417A and $0.65 \leq z \leq 1$ in Hole 417D.

SUMMARY AND CONCLUSIONS

Examination of 98 polished sections, determination of 74 Curie temperatures, and 11 microprobe analyses have confirmed that, as expected from models of increasing oxidation away from the ridge axis, the magnetic minerals of the Site 417 Cretaceous submarine basalts exhibit a largely developed low temperature oxidation.

Unlike in Leg 37, where Bleil and Petersen (1977) observed a decrease of cation deficiency with increasing depth, in Hole 417D a general but slight opposite trend is recorded by the Curie points through a thickness of about 400 meters, from the basement top down to the beginning of the dike injection zone, both in the pillows and in the massive units. If this trend is significant, it agrees better with the model proposed by Irving (1970) in which maghemitization increases with depth as a result of mild hydrothermal conditions that prevail in the buried flows of the rift valley. Subsequent to spreading and faulting of the crust, basalts of the superficial part of Layer 2 are likely to undergo further low temperature oxidation, depending on the time they have

been exposed to sea water weathering (halmyrolysis oxidation, Hart, 1973) and also upon the physical characteristics of the rocks (porosity, joint pattern, etc). As already mentioned by several authors (Ade-Hall et al., 1976b; Ryall et al., 1977; Bleil and Petersen, 1977; Marshall, 1978), sea water weathering is found to affect preferentially the pillows rather than the massive units; simply for emplacement mode and geometrical feature reasons, the circulating water has easier access to the pillows than to the massive units. This is actually observed at Site 417 where the pillows are generally more oxidized than the massive units.

In contrast to subaerial basalts, deuteric oxidation has rarely been observed in ocean floor basalts. The high temperature oxidation can only develop if the H_2 from dissociated water vapor can be lost from a cooling flow (Sato and Wright, 1966); this condition is hindered by the high confining pressures of deep ocean environment that considerably reduces gas loss from a cooling submarine flow.

In the massive units of Site 417, ilmenite exsolutions seldom have been observed, indicating that deuteric oxidation has been limited to local zones, probably around joints where hot fluid circulation was favored. Where observed, high temperature oxidation never exceeds class 3 of the six class scale of Watkins and Haggerty (1967). If the exsolved titanomagnetites were representative of the magnetic minerals population, their composition should be those of Ti-poor titanomagnetites with low values of x and high Curie points (450° - 580° C). In contrast, our data clearly indicate that the dominant magnetic mineral in the massive units is a Ti-rich titanomagnetite with variable degree of cation deficiency, the original stoichiometric titanomagnetite of which had an average composition typical of submarine basalts (x around 0.6). In fact, in the widespread massive unit samples including two generations of magnetic minerals, some of the early crystallized large titanomagnetites may have undergone deuteric oxidation before the population of small titanomagnetites (with x around 0.6) crystallized upon quenching of the residual liquid, the cooling conditions preventing the magnetic minerals from being exsolved.

Although the Curie temperatures and the microprobe analyses data do not show a significant difference between the average oxidation degrees in the massive units of both holes, it can be noted that the freshest, close to stoichiometric titanomagnetites are found in massive unit samples of Hole 417A. Possibly the abundance of secondary minerals in Hole 417A (calcite, smectites, etc) crystallized early within the veins of the basaltic units, providing an efficient screen against fluid circulations and preventing the titanomagnetites from being oxidized.

In the pillows, low temperature oxidation prevails everywhere, and the extreme values of the oxidation parameter are $0.6 \leq z \leq 1$, if we assume the same chemical conditions as in the massive units for the original titanomagnetite ($x = 0.6$ and $Al = 0.1$ at/formula unit). The average Curie temperatures are not significantly different in Holes 417A and 417D. This is somewhat unexpected because the whole pillow sequence was found to be strongly altered hydrothermally in Hole 417A, and in contrast, remarkably fresh in Hole 417D. It appears that the magnetic minerals behave differently from the silicates, being one of the first minerals to undergo alteration; they reach their equilibrium state

early which is to be a cation-deficient spinel in a sea water environment (Sakamoto et al., 1968), and later on after burial (Readman and O'Reilly, 1972).

Finally, according to previous observations (Ade-Hall et al., 1976a), no titanomagnetite alteration products as patches of rutile or anatase granules that commonly occur in zeolite facies of subaerial lavas are noticed. To be formed from a cation-deficient titanomagnetite, these minerals require a temperature of about 250° to 300° C, above which unmixing of the titanomaghemite occurs (Readman and O'Reilly, 1970).

Microscopic examination, Curie temperatures, and electron microprobe analyses of the magnetic minerals at Site 417 therefore do not show evidence for thermal events having occurred at temperatures above 250° C after the basalt emplacement. Rather, they favor the hypothesis that only mild hydrothermal metamorphism and/or halmyrolysis oxidation have prevailed since the cooling of this upper part of layer 2, a necessary condition for cation-deficient phases to be preserved.

ACKNOWLEDGMENTS

We wish to thank B. Koslowski and A. Salamon for their assistance in the laboratory work and M. Prévot for critically reading the manuscript.

The financial support by the Deutsche Forschungsgemeinschaft and by the Centre National pour l'Exploration des Océans is gratefully acknowledged.

REFERENCES

- Ade-Hall, J.M., Fink, L.K., and Johnson, H.P., 1976a. Petrography of opaque minerals, Leg 34. In Yeats, R.S., Hart, S.R., et al., *Initial Reports of the Deep Sea Drilling Project*, v. 34: Washington (U.S. Government Printing Office), p. 349-362.
- Ade-Hall, J.M., Johnson, H.P., and Ryall, P.J.C., 1976b. Rock magnetism of basalts, Leg 34. In Yeats, R.S., Hart, S.R., et al., *Initial Reports of the Deep Sea Drilling Project*, v. 34: Washington (U.S. Government Printing Office), p. 459-468.
- Akimoto, S., Katsura, T., and Yoshida, M., 1957. Magnetic properties of the Fe_2TiO_4 - Fe_3O_4 system and their change with oxidation, *J. Geomag. Geoelect.*, v. 9, p. 165-178.
- Bleil, U., 1971. Cation distribution in titanomagnetites, *Z. Geophys.*, v. 37, p. 305-319.
- Bleil, U. and Petersen, N., 1977. Magnetic properties of basement rocks, Leg 37, Site 332. In Aumento, F., Melson, W.G., et al., *Initial Reports of the Deep Sea Drilling Project*, v. 37: Washington (U.S. Government Printing Office), p. 449-456.
- , in press. Rock and paleomagnetism of Leg 43 basalts. In Tucholke, B., Vogt, P., et al., *Initial Reports of the Deep Sea Drilling Project*, v. 43: Washington (U.S. Government Printing Office).
- Buddington, A.F. and Lindsley, D.H., 1964. Iron-Titanium oxide minerals and synthetic equivalents, *J. Petrol.*, v. 5, p. 310-357.
- Evans, M.E. and Wayman, M.L., 1972. The Mid-Atlantic Ridge near 45° N. XIX. An electron microprobe investigation of the magnetic minerals in basalt samples, *Canadian J. Earth Sci.*, v. 9, p. 671-678.
- Ghorbanian, J., 1966. Sur les propriétés magnétiques des titanomagnétiques, Thèse, Université de Paris, p. 26-27.
- Haggerty, S.E., 1976. Oxide minerals, *Mineralogical Society of America Short Course Notes*, Chapter 4, p. Hg 1-Hg 28 and Chapter 8, p. Hg 101-Hg 109.

- Hart, R.A., 1973. A model for chemical exchange in the basalt seawater system of oceanic Layer 2, *Canadian J. Earth Sci.*, v. 10, p. 799-816.
- Irving, E., 1970. The Mid-Atlantic Ridge at 45°N. XIV. Oxidation and magnetic properties of basalt; review and discussion, *Canadian J. Earth Sci.*, v. 7, p. 1528-1538.
- Jensen, S.D. and Shive, P.N., 1973. Cation distribution in sintered titanomagnetites, *J. Geophys. Res.*, v. 78, p. 8474-8480.
- Marshall, M., 1978. The magnetic properties of some DSDP basalts from the North Pacific and inferences for Pacific plate tectonics, *J. Geophys. Res.*, v. 83, p. 289-308.
- Nagata, T., 1961. *Rock Magnetism*. Tokyo (Maruzen Company Ltd.), p. 46-49.
- O'Donovan, J.B. and O'Reilly, W., 1977. The preparation, characterization and magnetic properties of synthetic analogues of some carriers of the paleomagnetic record, *J. Geomag. Geoelectr.*, v. 29, p. 331-344.
- O'Reilly, W. and Banerjee, S.K., 1967. The mechanism of oxidation in titanomagnetites: A magnetic study, *Min. Mag.*, v. 36, p. 29-37.
- O'Reilly, W. and Readman, P.W., 1971. The preparation and unmixing of cation deficient titanomagnetites, *Z. Geophys.*, v. 37, p. 321-327.
- Ozima, M. and Sakamoto, N., 1971. Magnetic properties of synthesized titanomaghemites, *J. Geophys. Res.*, v. 76, p. 7035-7046.
- Ozima, M., Joshima, M., and Kinoshita, H., 1974. Magnetic properties of submarine basalts and the implications on the structure of the oceanic crust, *J. Geomag. Geoelectr.*, v. 26, p. 335-354.
- Petersen, N., Bleil, U., and Eisenack, P., 1978. Rock and paleomagnetism of Leg 42A basalts. In Hsü, K.T., Montadert, L., et al., *Initial Reports of the Deep Sea Drilling Project*, v. 42, Part 1: Washington (U.S. Government Printing Office), p. 881-886.
- Prévot, M. and Lecaille, A., 1976. Sur le caractère épisodique du fonctionnement des zones d'accrétion: critique des arguments géomagnétiques, *Bull. Soc. Géol. France*, v. 18, p. 903-911.
- Prévot, M., Remond, G., and Caye, R., 1968. Etude de la transformation d'une titanomagnétite en titanomaghémite dans une roche volcanique, *Bull. Soc. Fr. Minéral. Cristallogr.*, v. 91, p. 65-74.
- Readman, P.W. and O'Reilly, W., 1970. The synthesis and inversion of nonstoichiometric titanomagnetites, *Phys. Earth Planet. Int.*, v. 4, p. 121-128.
- , 1972. Magnetic properties of oxidized (Cation-deficient) titanomagnetites (Fe, Ti, □)₃O₄, *J. Geomag. Geoelectr.*, v. 24, p. 69-90.
- Richard, J.C.W., O'Donovan, J.B., Hauptman, Z., O'Reilly, W., and Creer, K.M., 1973. A magnetic study of titanomagnetite substituted by magnesium and aluminum, *Phys. Earth Planet. Int.*, v. 7, p. 437-444.
- Ryall, P.J.C., Hall, J.M., Clark, J., and Milligan, T., 1977. Magnetization of oceanic crustal Layer 2; results and thoughts after DSDP Leg 37, *Canadian J. Earth Sci.*, v. 14, p. 684-706.
- Sakamoto, N., Ince, P.I., and O'Reilly, W., 1968. The effect of wet-grinding in the oxidation of titanomagnetites, *Geophys. J. Roy. Astron. Soc.*, v. 15, p. 509-515.
- Sato, M. and Wright, T.L., 1966. Oxygen fugacities directly measured in magmatic gases, *Science*, v. 153, p. 1103-1105.
- Watkins, N.D. and Haggerty, S.E., 1967. Primary oxidation variation and petrogenesis in a single lava, *Contrib. Mineral. Petrol.*, v. 15, p. 251-271.